Proceedings of the 2007 American Control Conference
Marriott Marquis Hotel at Times Square
New York City, USA, July 11-13, 2007

Nonholonomic robots navigation using linear navigation functions

Fethi Belkhouche

Texas A&M Intl University
Texas, 78041
Email: fbelkhouche@tamiu.edu

Abstract— **In this paper we suggest a new navigation strategy for nonholonomic wheeled mobile robots. The method is based on linear navigation functions with exponential and deviation terms. These linear navigation functions are based on the kinematics equations and the geometry of the navigation problem, where the robot's orientation angle is a linear function of the visibility angle. Another control law is suggested for the robot's linear velocity. This approach allows driving the robot from an initial configuration to a desired final configuration. The robot's orientation angle depends on four different parameters that allow to change the robot path in real time. The navigation functions are combined with a collision avoidance algorithm to avoid obstacles. The approach is illustrated using various simulation examples.**

I. Introduction

Navigation is among the most important functions in robotics. Navigation is necessary to accomplish different tasks. Various navigation methods are discussed in the literature. The potential field method is among the most discussed methods in the robotics community. This method was initially suggested in 1986 for robotic manipulators [1]. In the potential field method, the robot moves in a field that combines repulsive forces resulting from the obstacles and an attractive force resulting from the goal. Unfortunately, the potential field method suffers from the problem of local minima. Different approaches have been suggested to solve this problem. Recently, a modified Newton's method was suggested in [2], where C^2 continuous navigation functions are defined. This improves the system's performance compared to the classical approach of the potential field method. A vectorial approach to the potential field method is suggested in [3]. The artificial vector potential field shows a better ability to steer motion than does a scalar potential field. In [4], an electrostatic potential field is suggested. It is proven through the classical laws of electrostatics that the derived potential function is a global navigation function, and that the field is free of all local minima and that all paths necessarily lead to the goal position. The virtual force field (VFF) suggested by Borenstein and Koren [5] combines the histogram grid world model with the concept of potential fields. This method suffers from drawbacks that are inherited to the potential field method. The authors also suggested the vector field histogram (VHF) method [6], which uses a two dimensional Cartesian histogram grid to model the word. This histogram is then reduced to a polar histogram representing the polar obstacles density in a given direction.

Various sensor-based navigation methods are used for robot navigation, where different types of sensors are used [7], [8]. Vision sensors are the most used sensors [9], [10], [11], [12]. In [13] a method for visual-based navigation with a single omni-directional camera is described. In [14], central and peripheral vision methods are combined for reactive robot navigation. Monocular vision is used for robot navigation in [15], where a three dimensional map of the trajectory and the environment is constructed. A fast algorithm for robot vision-based robot navigation is suggested in [16], where visual sensors are mainly used for mapping. In [10], vision and odometry are combined together to accomplish the navigation task. A survey on methods using vision for robot navigation can be found in [17].

In [8], sensing and planning functions are combined together to produce active sensing. A multi-sensor approach is suggested in [18], where vision and sonar-based strategies are combined together.

The problem of nonholonomic navigation is more difficult because of the nonholonomic constraint. Under the nonholonomic constraint, the robot cannot turn without changing its coordinates. Different methods are suggested to navigate a wheeled mobile robot from its initial configuration to a final configuration under the nonholonomic constraints [18], [19], [20]. Our goal in this paper is to contribute to solve the problem of nonholonomic robot's navigation in the presence of obstacles. We suggest a new family of navigation functions for nonholonomic wheeled mobile robots navigation. Our navigation functions are different from the classical navigation functions defined in terms of the potential field or other methods. Here the robot orientation angle is a linear continuous function of the visibility angle. In this paper, we restrict ourselves to stationary obstacles. Moving obstacles can be considered by taking into acount the relative kinematics between the robot and the obstacle. In the next section, we introduce several important definitions.

II. Preliminaries

As we mentioned previously, our approach is based on the geometric rules and the kinematics equations. In this section, we define the geometric quantities that characterize the navigation problem and we derive the kinematics model. With reference to figure 1, the visibility line is the imaginary straight line that starts at the reference point of the robot and is directed towards the goal. The angle δ is called here

1-4244-0989-6/07/$25.00 ©2007 IEEE.

the visibility angle. δ is defined as the angle between the reference line parallel to the positive x-axis and visibility line. The robot's kinematics model is given by

$$\begin{aligned} \dot{x} &= v\cos\theta \\ \dot{y} &= v\sin\theta \\ \dot{\theta} &= \omega \end{aligned} \tag{1}$$

where (x, y) denote the coordinates of the robot's reference point; θ is the robot's orientation angle. (v, ω) represent the linear and angular velocities of the robot. The position of the goal in the Cartesian frame of reference is given by (x_G, y_G). The kinematics model given by 1 gives the motion of a wheeled mobile robot of the unicycle type, and it captures the nonholonomic constraint. In this paper the control input is (v, θ) instead of (v, ω). The relative distance between the robot's reference point and the goal is given by r. Here we suggest to use polar coordinates. We first define the relative velocity in the Cartesian frame of coordinates between the robot and the goal as follows

$$\begin{aligned} \dot{x}_{rel} &= -\dot{x} \\ \dot{y}_{rel} &= -\dot{y} \end{aligned} \tag{2}$$

where x_{rel} and y_{rel} are given by

$$x_{rel} = x_G - x, y_{rel} = y_G - y \tag{3}$$

Equations (1) and (2) give

$$\begin{aligned} \dot{x}_{rel} &= -v\cos\theta \\ \dot{y}_{rel} &= -v\sin\theta \end{aligned} \tag{4}$$

By using the following transformation of coordinates

$$\begin{aligned} x_{rel} &= r\cos\delta \\ y_{rel} &= r\sin\delta \end{aligned} \tag{5}$$

we obtain the equivalent polar kinematics model given by

$$\begin{aligned} \dot{r} &= -v\cos(\theta - \delta) \\ \dot{\delta} &= -vr^{-1}\sin(\theta - \delta) \end{aligned} \tag{6}$$

Clearly

$$\begin{aligned} r &= \sqrt{x_{rel}^2 + y_{rel}^2} \\ \delta &= a\tan 2\,(y_{rel}, x_{rel}) \end{aligned} \tag{7}$$

The kinematics model given by (6) describes the relative motion between the robot and its goal. The first equation gives the relative distance, the second equation gives the rate of turn of the robot with respect to the goal. Clearly $\dot{r} < 0$ corresponds to the robot approaching from its goal, and $\dot{\delta} = 0$ corresponds to the robot moving in a straight line.

III. Approach

Kinematics-based navigation functions were recently suggested to navigate wheeled mobile robots towards a given goal in the presence of obstacles [21], [22]. In this paper we suggest to use linear navigation functions to drive a wheeled mobile robot from an initial configuration given by (x_0, y_0, θ_0) to a final configuration given by (x_f, y_f, θ_f). There exists a nonholonomic constraint on the robot turning radius. This constraint must be taken into account. Our

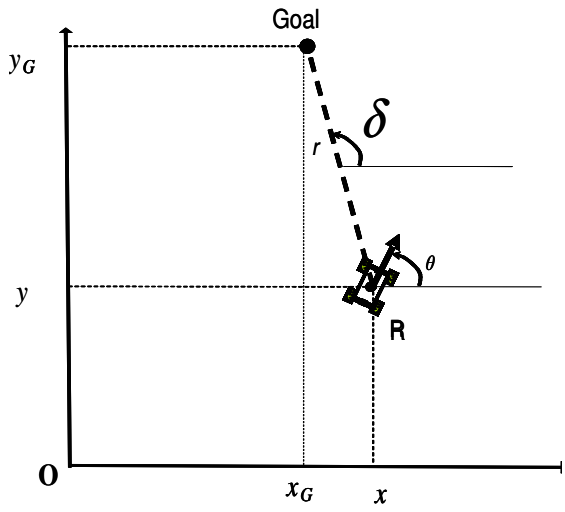

Fig. 1. Geometry of the navigation problem

control input for the robot's orientation angle is given by

$$\theta = B\delta + b_0 e^{-at} + b_1 \tag{8}$$

where B is a constant real number called the proportionality constant, with $B \geq 1$; b_0 and b_1 are angles characterizing the initial state and the final state of the robot's orientation angle, respectively; a is a real positive number. B, a, b_0 and b_1 are called the navigation parameters. They allow to control the robot's path. As it can be seen from equation (8), the control input for the robot's orientation angle has three terms: a proportionality term, which is the most important term, an exponential term and a deviation term. The exponential term is used for heading regulation. The initial value of the robot's orientation angle is given by

$$\theta_0 = B\delta_0 + b_0 + b_1 \tag{9}$$

The control input for the robot's linear velocity is given by

$$v = Kr \tag{10}$$

K is another proportionality factor with $K > 0$. There is a constraint on K, where

$$K < \frac{v_{max}}{r_{max}} \tag{11}$$

where v_{max} and r_{max} are the maximum values of v and r, respectively. In general $r_{max} = r_0$. Equation (10) shows that the robot linear velocity is proportional to the relative distance robot-goal. Clearly, according to the linear velocity control law, the robot slows down when it gets closer to the goal, and comes to a full stop when it reaches the goal. Under the control law, the closed loop system is given by

$$\begin{aligned} \dot{r} &= -Kr\cos\left((B-1)\,\delta + b_0 e^{-at} + b_1\right) \\ \dot{\delta} &= -K\sin\left((B-1)\,\delta + b_0 e^{-at} + b_1\right) \end{aligned} \tag{12}$$

The dynamics of this kinematics model characterize the robot motion in the polar plane (r, δ).

Proposition 1: As $t \to \infty$, the equilibrium positions for the visibility angle rate equation are given by

$$\delta_{eq}^1 = \frac{-b_1}{B-1} \quad (13)$$

$$\delta_{eq}^2 = \frac{-b_1}{B-1} \pm n\pi \quad (14)$$

where n is an integer, $n = 1, 2...$

Proof:

An equilibrium position for the visibility angle rate equation satisfies $\dot{\delta} = 0$. From equation (12), this corresponds to

$$\sin\left((B-1)\,\delta + b_0 e^{-at} + b_1\right) = 0 \quad (15)$$

From which it turns out that

$$\delta_{eq}^1 = \frac{-b_1 - b_0 e^{-at}}{B-1} \quad (16)$$

and

$$\delta_{eq}^2 = \frac{-b_1 - b_0 e^{-at}}{B-1} + n\pi \quad (17)$$

As $t \to \infty$, the values of δ_{eq}^1 and δ_{eq}^2 are similar to equations (16) and (17). The final value for the robot's orientation angle corresponding to δ_{eq}^1 is given by

$$\theta_f = \frac{-b_1}{B-1} \quad (18)$$

■

Our main result can be stated as follows.

Proposition 2: Under the control laws given by (8) and (10), the robot reaches successfully its goal with a final orientation angle

$$\theta_f = \frac{-b_1}{B-1} \quad (19)$$

Proof:

The proof that the robot reaches the goal position is based on the kinematics equations, where the goal is to prove that the equilibrium position given by $\left(0, \delta_{eq}^1\right)$ is an asymptotically stable equilibrium position for system (12). Now, in order to prove that this equilibrium position is asymptotically stable, we use the classical linearization theorems. The classical linearization near the equilibrium position is given by

$$A = \begin{bmatrix} -K & 0 \\ 0 & -K \end{bmatrix} \quad (20)$$

The eigenvalues of A are negative, which means that the equilibrium position $\left(0, \delta_{eq}^1\right)$ is asymptotically stable, thus $r \to 0$, and $\delta \to \delta_{eq}^1$. As a result, the final value of the robot's orientation angle is given by $\theta_f = \frac{-b_1}{B-1}$. In a similar way, it is possible to prove that δ_{eq}^2 is unstable.

■

The most important property of our control-navigation law is the possibility to change the path using the proportionality factor B. In most cases b_0 and b_1 are chosen to satisfy the conditions on the initial and final orientation angles. The real number a characterizes the turning radius. Smaller values of a correspond to wider turns. This is illustrated in figure 2 for different values of a.

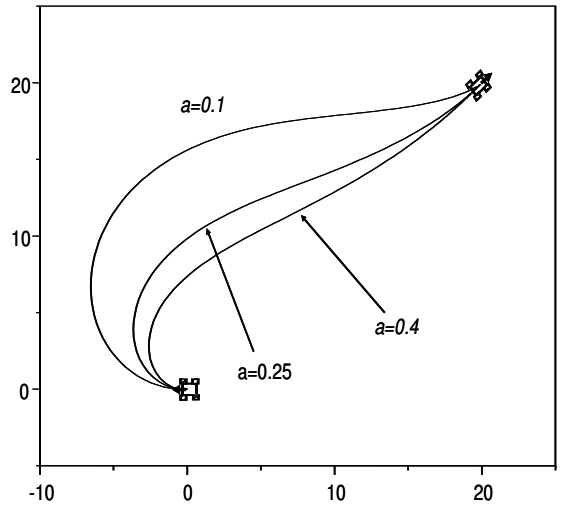

Fig. 2. Influence of a on the robot's path and turning radius

IV. Collision avoidance

The problem of collision avoidance becomes more difficult under the nonholonomic constraint. In this case, collision is avoided by changing the values of the navigation parameters or by navigating towards an intermediary goal. For collision avoidance, our method is combined with the beam method, where the goal is to get the local heading based on angular information to obtain free path by changing the value of B. The beam method allows to obtain an angular description of the environment based on the sensory system. Each obstacle O_b is defined by three parameters ρ_1, ρ_2 and d, where ρ_1 and ρ_2 are the limit angles from the positive x-axis as shown in figure 3; d is the distance robot-obstacle. We will write $O_b\left(\rho_1, \rho_2, d\right)$. From figure 3, the angles ρ_1, ρ_2 are given by

$$\rho_1 = a\tan 2\left(y_{L1} - y, x_{L1} - x\right) \quad (21)$$

$$\rho_2 = a\tan 2\left(y_{L2} - y, x_{L2} - x\right) \quad (22)$$

where (x_{Li}, y_{Li}) are the coordinates of the points L_i as shown in figure 3.

It is worth noting that only obstacles within a given region are considered in the collision avoidance algorithm. Also the distance d_{min} to activate the collision avoidance algorithm must be large enough to take into account for the robot turning radius and dynamic constraints. In our collision avoidance algorithm, the robot slows down near collision. A control law similar to equation 10 is used. Collision avoidance is accomplished by navigation towards one of the intermediary goals G_1 or G_2 as shown in figure 3. The visibility angles between the robot and the intermediary goals G_1 and G_2 are given by δ_{G1} and δ_{G2}, respectively. In order to avoid the collision, the robot moves according to

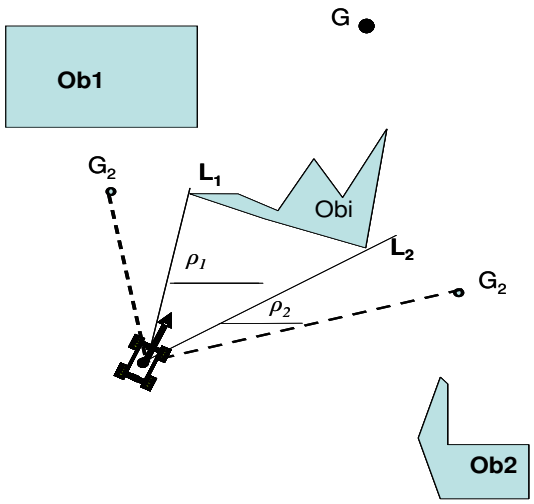

Fig. 3. Collision avoidance

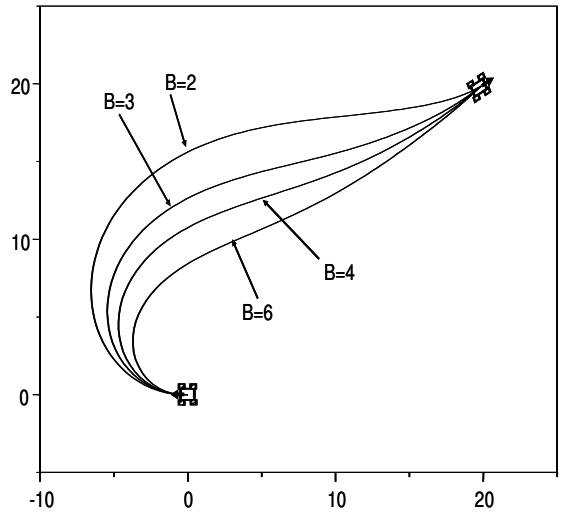

Fig. 4. Robot navigation for different values of B

the following control law

$$\theta = B\delta_{Gi} + b_0 e^{-at} + b_1 \tag{23}$$

with $i = 1, 2$. The smoothness of the path must be preserved when the robot switches to the collision avoidance mode. Let $\theta_0^{t_i}$ be the robot's orientation angle at time t_i when the robot starts deviation from the obstacle (t_i characterizes the beginning of the collision avoidance mode). The navigation parameters in the collision avoidance mode are chosen to satisfy

$$\theta_0^{t_i} = B\delta_{Gi}(t_i) + b_0 + b_1 \tag{24}$$

which guarantees the smoothness of the path. The navigation parameters are calculated online to navigate the robot towards the intermediary goals. These goals are chosen based on the sensory data. in [23] Q–learning is used to fix the navigation parameters. We restrict ourselves to stationary. However, moving obstacles can be considered too. This task can be accomplished by considering relative kinematics equations between the robot and the obstacles.

V. Simulation

We present a few simulation examples in the absence and presence of obstacles. In the example of figure 4, the robot initial configuration is given by $(20, 20, \pi)$. The aim is to drive the robot to a final configuration given by $\left(20, 20, \frac{\pi}{4}\right)$. As shown in figure 4, this task is accomplished successfully by using linear navigation functions for different values of B. The scenario of figure 5 is similar but with a final configuration $\left(20, 20, \frac{\pi}{2}\right)$. It is clear that different values of B result in different paths. The scenarios of figures 6 and 7 show navigation in the presence of obstacles. The robot's initial configuration is $(20, 20, \pi)$, and the final configuration is $\left(20, 20, \frac{\pi}{2}\right)$. Two different paths are accomplished by the robot by using different values of B.

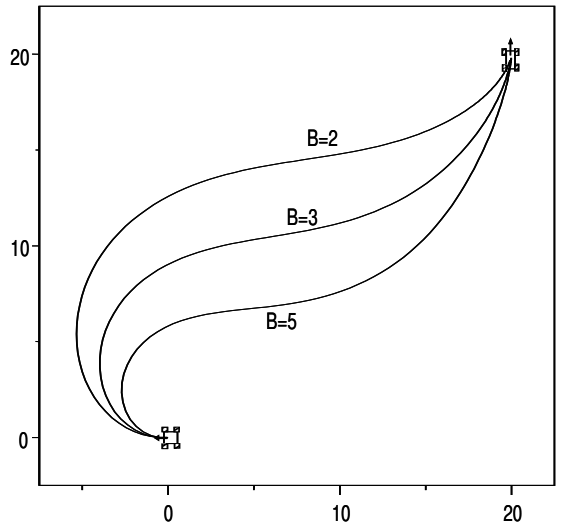

Fig. 5. Robot navigation for different values of B

VI. Conclusion

In this paper we suggested a method for navigation of nonholonomic wheeled mobile robots. The method is based on linear navigation functions, where the robot's orientation angle is proportional to the visibility angle between the robot and its goal. Our navigation law depends on four control parameters, and the path of the robot is different for different combinations of the values of these parameters. The same control law is used in the collision avoidance mode to navigate the robot towards an intermediary goal. A second control law is derived for the robot's linear velocity, where the robot slows down near obstacles and in sharp turns. The

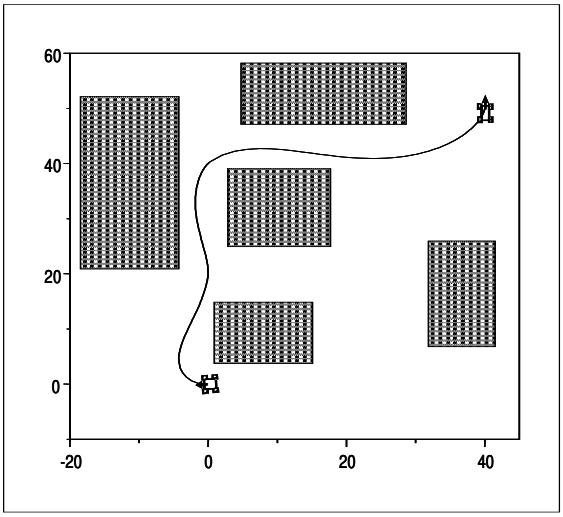

Fig. 6. Robot's path in the presence of obstacles

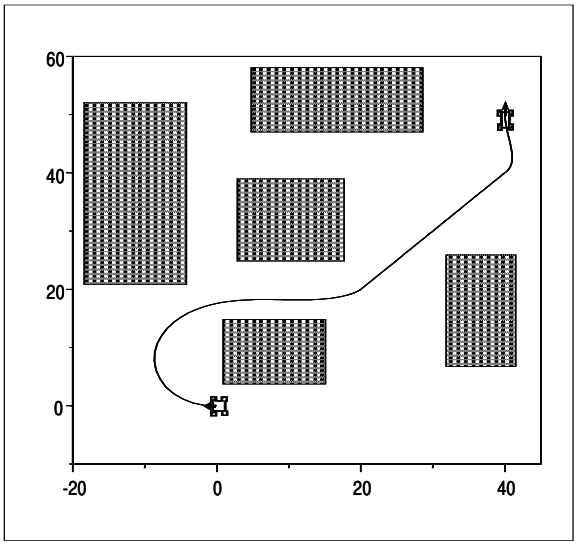

Fig. 7. Robot's path in the presence of obstacles

algorithm allows to drive the robot from an arbitrary initial configuration to a desired final configuration. Our results are mathematically proven and the method is illustrated using an extensive simulation.

REFERENCES

[1] O. Khatib, "Real-time obstacle avoidance for manipulators and mobile robots," *International Journal of Robotics Research*, vol. 5, no. 1, pp. 90–98, 1986.

[2] J. Ren, K. Mcisaac, and V. Patel, "Modified newton's method applied to potential field-based navigation for mobile robots," *IEEE Transactions on Robotics*, vol. 22, no. 2, pp. 384–391, 2006.

[3] G. DeSouza and A. Kak, "Constrained motion control using vector potential fields," *IEEE Transactions on Systems, Man and Cybernetics, Part A*, vol. 30, no. 3, pp. 251–272, 2000.

[4] K. Valavanis, T. Hebert, R. Kolluru, and N. Tsourveloudis, "Mobile robot navigation in 2-d dynamic environments using an electrostatic potential field," *IEEE Transactions on Systems, Man and Cybernetics, Part A*, vol. 30, no. 2, pp. 187–196, 2000.

[5] J. Borenstein and Y. Koren, "Real-time obstacle avoidance for fast mobile robots," *IEEE Transactions on Systems, Man, and Cybernetics*, vol. 19, no. 5, pp. 1179–1187, 1989.

[6] ——, "The vector field histogram – fast obstacle-avoidance for mobile robots," *IEEE Journal of Robotics and Automation*, vol. 7, no. 3, pp. 278–288, 1991.

[7] A. Elfes, "Sonar-based real-world mapping and navigation," *IEEE Transactions on robotics and Automation*, vol. 3, no. 3, pp. 249–265, 1987.

[8] V. Lumelsky and T. Skewis, "Incorporating range sensing in the robot navigation function," *IEEE Transactions on Systems, Man and Cybernetics*, vol. 20, no. 5, pp. 1058–1069, 1990.

[9] J. Borenstein and Y. Koren, "Vision-based navigation by a mobile robot with obstacle avoidance using single-camera vision and ultrasonic sensing," *IEEE Journal of Robotics and Automation*, vol. 14, no. 6, pp. 969–978, 1998.

[10] C. Taylor and D. Kriegman, "Vision-based motion planning and exploration algorithms for mobile robots," *IEEE Journal of Robotics and Automation*, vol. 14, no. 3, pp. 417–426, 1998.

[11] Y. Ma, J. Kosecka, and S. Sastry, "Vision guided navigation for a nonholonomic mobile robot," *IEEE Journal of Robotics and Automation*, vol. 15, no. 3, pp. 521–536, 1999.

[12] C. Taylor and D. Kriegman, "Vision-based navigation and environmental representations with an omnidirectional camera," *IEEE Journal of Robotics and Automation*, vol. 16, no. 6, pp. 890–898, 2000.

[13] N. Winters, J. Gaspar, G. Lacey, and J.Santos-Victor, "Omnidirectional vision for robot navigation," in *Proc. IEEE International Conference on Omnidirectional Vision*, Head Island, SC, June 2000, pp. 21–28.

[14] A. Argyros and F. Bergholm, "Combining central and peripheral vision for reactive robot navigation," in *Proc. IEEE International Conference on Computer Vision and Pattern Recognition*, Fort Collins, CO, June 1999, pp. 651–655.

[15] E. Royer, J. B. M. Dhome, B. Thuilot, M. Lhuillier, and F. Marmoiton, "Outdoor autonomous navigation using monocular vision," in *Proc. IEEE International Conference on Intelligent Robots and Systems*, Aug. 2005, pp. 1253–1258.

[16] A. Howard and L. Kitchen, "Fast visual mapping for mobile robot navigation," in *Proc. IEEE International Conference on Intelligent Processing Systems*, Beijing, Oct. 1997, pp. 1251 – 1255.

[17] G. DeSouza and A. Kak, "Vision for mobile robot navigation: A survey," *IEEE Transactions on Pattern analysis and machine intelligence*, vol. 24, no. 2, pp. 237–267, 2002.

[18] C. Marques and P. Lima, "Avoiding obstacles - multisensor navigation for nonholonomic robots in cluttered environments," *IEEE Tobotics & Automation Magazine*, vol. 11, no. 3, pp. 70–82, 2004.

[19] S. Konkimalla, P. LaValle, "Efficient computation of optimal navigation functions for nonholonomic planning," in *Proc. Robot Motion and Control*, Kiekrz, 1999, pp. 187–192.

[20] S. Patel, J. Sang-Hack, J. Ostrowski, R. Rao, and C. Taylor, "Sensor based door navigation for a nonholonomic vehicle," in *Proc. IEEE International Conference on Robotics and Automation*, Washington, DC, May 2002, pp. 3081–3086.

[21] F. Belkhouche and B. Belkhouche, "Wheeled mobile robot navigation using the proportional navigation," *Advanced Robotics*, p. in press.

[22] F. Belkhouche, B. Belkhouche, and P. Rastgoufard, "Autonomous navigation and obstacle avoidance using navigation laws with time–varying deviation functions," *Advanced Robotics*, p. in press.

[23] F. Belkhouche and K. Bendjilali, "Q–learning of linear navigation functions," in *Proc. 5th International Conference on Industrical automation*, Montreal, June 2007, p. accepted.